SARS-CoV-2 induces inflammasome-dependent pyroptosis and downmodulation of HLA-DR in human monocytes, which can be prevented by atazanavir

André C. Ferreira[1,2,10#*], Vinicius Cardoso Soares[1,9#], Isaclaudia G. de Azevedo-Quintanilha[1], Suelen da Silva Gomes Dias[1], Natalia Fintelman-Rodrigues[1,10], Carolina Q. Sacramento[1,10], Mayara Mattos[1,10], Caroline S. de Freitas[1,10], Jairo R. Temerozo[3,4], Lívia Teixeira[1], Eugenio Damaceno Hottz[1,5], Ester A Barreto[1], Camila R. R. Pão[1], Lohanna Palhinha[1], Milene Miranda[6], Dumith Chequer Bou-Habib[3,4], Fernando A. Bozza[7,8], Patrícia T. Bozza[1] , Thiago Moreno L. Souza[1,10*]

1 – Laboratório de Imunofarmacologia, Instituto Oswaldo Cruz (IOC), Fundação Oswaldo Cruz (Fiocruz), Rio de Janeiro, RJ, Brazil.

2 – Universidade Iguaçu, Nova Iguaçu, RJ, Brazil.

3 – Laboratório de Pesquisas sobre o Timo, IOC, Fiocruz, Rio de Janeiro, RJ, Brazil.

4 – National Institute for Science and Technology on Neuroimmunomodulation, Oswaldo Cruz Institute, Fiocruz, Rio de Janeiro, RJ, Brazil.

5 – Laboratório de Imunotrombose, Departamento de Bioquímica, Universidade Federal de Juiz de Fora, Juiz de Fora, MG, Brazil.

6 – Laboratório de Vírus Respiratório e do Sarampo, IOC, Fiocruz, Rio de Janeiro, RJ, Brazil.

7 – Instituto Nacional de Infectologia Evandro Chagas, Fiocruz, Rio de Janeiro, RJ, Brazil.

8 – Instituto D'or de Pesquisa e Ensino, Rio de Janeiro, RJ, Brazil.

9 - Program of Immunology and Inflammation, Federal University of Rio de Janeiro, UFRJ, Rio de Janeiro, RJ, Brazil.

10 - Centro De Desenvolvimento Tecnológico Em Saúde (CDTS), Fiocruz, Rio de Janeiro, Brasil.

# These authors contributed equally to this work

* corresponding author

Abstract

Infection by the severe acute respiratory syndrome coronavirus 2 (SARS-CoV-2) has been associated with leukopenia and uncontrolled inflammatory response in critically ill patients. A better comprehension of SARS-CoV-2-induced monocytes death is essential for the identification of therapies capable to control the hyper-inflammation and reduce viral replication in patients with COVID-19. Here, we show that SARS-CoV-2 induces inflammasome activation and cell death by pyroptosis in human monocytes, experimentally infected and in patients under intensive care. Pyroptosis was dependent on caspase-1 engagement, prior to IL-1ß production and inflammatory cell death. Monocytes exposed to SARS-CoV-2 downregulate HLA-DR, suggesting a potential limitation to orchestrate the immune response. Our results originally describe the mechanism by which monocytes, a central cellular component recruited from peripheral blood to respiratory tract, succumb in patients with severe 2019 coronavirus disease (COVID-19), and emphasize the need for identifying anti-inflammatory and antiviral strategies to prevent SARS-CoV-2-induced pyroptosis.

Introduction

Severe acute respiratory coronavirus 2 (SARS-CoV-2), the etiological agent of the 2019 coronavirus disease (COVID-19), emerged in China, causing a major public health burden in decades. Patients with COVID-19 may develop an asymptomatic or mild disease or be affected by the life threatening acute respiratory distress syndrome (ARDS), which is characterized by elevated serum levels of proinflammatory mediators, the cytokine storm (1-3). In the respiratory tract of patients with severe COVID-19, monocytes/macrophages may be the main source of uncontrolled levels of the pro-inflammatory mediators TNF-α and IL-6 (4). Plasmatic levels of IL-6 have been associated with mortality, intensive care admission and hospitalization, representing a poor prognostic factor for COVID-19 (5). The uncontrolled inflammation promoted by SARS-CoV-2 in severe COVID-19 is not acute, it negatively associates with viral loads in nasopharyngeal swabs and represents an important event from 7 to 10 days after onset of illness (6-7). Along with uncontrolled pro-inflammatory response, severe COVID-19 associates with high levels of tissue insult, judged by increased levels of lactate dehydrogenase (LDH) and D-dimer in the plasma and leukopenia (6-8). In addition, a

severe immune dysregulation with low antigen presenting capacity is evidenced by reduced expression of HLA-DR in monocytes during COVID-19, which is strongly associated with severe respiratory failure (4).

The leucopenia and increased LDH levels in the plasma of patients with severe COVID-19 seem to precede the cytokine storm (9-14). Moreover, in other virus-induced cytokine storm episodes in the respiratory tract, such as induced by influenza A virus, monocytes and macrophages are severely affected (9). We thus hypothesized that SARS-COV-2-induced cell death of monocytes could impair a resolutive cytokine release. Indeed, we found that SARS-CoV-2 triggers inflammasome activation, leading to pyroptosis in human monocytes, either by experimental or natural infection. Pyroptosis was dependent on caspase-1 engagement, prior to IL-1ß production and dysregulation of cytokine release. Monocytes that survive after SARS-CoV-2 challenge downregulate HLA-DR, being less likely to properly orchestrate the immune response. Finally, we show that the reproposed antiviral drugs atazanavir could block this deleterious loop in favor of the host.

Material and Methods

Reagents

Atazanavir (ATV) and Ribavirin were received as donations from Instituto de Tecnologia de Fármacos (Farmanguinhos, Fiocruz). The antiviral Lopinavir/ritonavir (4:1 proportion) was pruchased from AbbVie (Ludwingshafen, Germany). ELISA assays were purchased from R&D Bioscience. Lipopolysacchadides - LPS, adenosine triphosphate (ATP), the specific inhibitor of caspase-1 (AC-YVAD-CMK), pan-caspase inhibitor (ZVAD-FMK), RIPK1 (Necrostatin-1 – Nec-1) and IL-1 receptor (IL-1RA) were all purchased from Sigma-Aldrich (St. Louis, MO, USA). All small molecule inhibitors were dissolved in 100 % dimethylsulfoxide (DMSO) and subsequently diluted at least 10^4-fold in culture or reaction medium before each assay. The final DMSO concentrations showed no cytotoxicity. The materials for cell culture were purchased from Thermo Scientific Life Sciences (Grand Island, NY), unless otherwise mentioned.

94 **Cells and Virus**

95 African green monkey kidney (Vero, subtype E6) cells were cultured in DMEM
96 high glucose supplemented with 10 % fetal bovine serum (FBS; HyClone, Logan, Utah)
97 and 100 U/mL penicillin, and 100 µg/mL streptomycin (P/S). Vero cells were incubated
98 at 37°C in 5 % CO_2 atmosphere.

99 Human primary monocytes were obtained through plastic adherence of peripheral
100 blood mononuclear cells (PBMCs), which were obtained from buffy coat preparations of
101 healthy donors by density gradient centrifugation (Ficoll-Paque, GE Healthcare). In brief,
102 PBMCs (2.0 x 10^6 cells) were plated onto 48-well plates (NalgeNunc) in RPMI-1640
103 without serum for 2 to 4 h; then, non-adherent cells were removed by washing and the
104 remaining monocytes were maintained in DMEM with 5% human serum (HS; Millipore)
105 and penicillin/streptomycin.

106 SARS-CoV-2 was isolated and expanded on Vero E6 cells from a nasopharyngeal
107 swab of a confirmed case from Rio de Janeiro, Brazil. Experiments were performed after
108 one passage in cell culture, when Vero E6 cells with DMEM plus 2% FBS in 150 cm^2
109 flasks were incubated at 37 °C in 5 % CO_2 atmosphere. Cytopathic effect was observed
110 daily and peaked 4 to 5 days after infection. All procedures related to virus culture were
111 handled at biosafety level 3 (BSL3) multiuser facility, according to WHO guidelines.
112 Virus titers were determined as the tissue culture infectious dose at 50% (TCID50/mL).
113 Virus stocks were kept in -80 °C ultralow freezers. The virus strain was sequenced to
114 confirm the virus identity and its complete genome is publicly deposited (GenBank
115 accession no. MT710714).

116 **Yield-reduction assay**

117 Human primary monocytes were infected with multiplicity of infection (MOI) of
118 0.01 at density of 2-8 x 10^5 cells/well in 48-well culture plates, depending on the total cell
119 number from each donor. After 1 h at 37 °C, cells were washed, and various
120 concentrations of compounds were added in DMEM with 2% FBS. After 48 h, the
121 supernatants were harvested and virus replication was quantified by real time RT- PCR
122 and infectious titers by TCID50/mL.

123 **Virus titration**

124 Monolayers of Vero cells (2 x 10^4 cell/well) in 96-well culture plates were infected
125 with log- based dilutions of the supernatants containing SARS-CoV-2 for 1 h at 37°C.
126 The cells were washed and fresh medium with 2% FBS was added. After 3 to 5 days, the
127 cytopathic effects were scored in at least 10 replicates per dilution by independent readers,
128 who were blind with respect to source of the supernatant. Reed and Muench scoring
129 method was employed to determine TCID50/mL.

130 **Flow cytometer analysis**

131 For flow cytometry analysis, monocytes were diluted in labelling buffer (10^6
132 cells/mL). Then, 100 µL of cell samples were marked with 5 µL of AnnexinV and PI for
133 15 minutes for cell death evaluation. Around 10,000 gated events were acquired using
134 FACSCalibur and the analysis was performed using the CellQuest software. Monocytes
135 were gated through cell size (foward light scatter, FSC) and granularity (side light scatter,
136 SSC) analysis.

137 Human monocytes were stained for caspase-1 activity with FAM-YVAD-FMK
138 (fluorescent-labeled inhibitor of caspase-1 [FLICA] and FAM-FLICA Caspase-3/7
139 activity or HLA-DR APC.H7 or IgG APC.H7. Caspase-1 and caspase-3/7 activity was
140 determined via flow cytometry (FACSCalibur) by detecting FLICA fluorescence and
141 expression of HLA-DR as mean fluorescence intensity (MFI) value for each sample.
142 Acquisition of data was set to count a total of 10,000 events, and the FLOWJO software
143 package was used to analyze the data.

144 **Microscopic analysis**

145 Human primary monocytes were plated on glass coverslips at density of 2-8 x 10^5
146 cells/well in 48-well plates. Infection was performed for 2 h at 37 °C and then fresh
147 medium with 2% FBS was added. After 24 h, the cells were washed with Binding buffer
148 and stained with PI (0.5 µg/mL) for 5 minutes. Next, the cells were fixed with 3.7%
149 formaldehyde for 30 minutes at room temperature. The nuclei were stained with DAPI
150 (1µg/mL) for 5 min and the coverslips were mounted using an antifade mounting medium

151 (VECTASHIELD). Fluorescence was analyzed by fluorescence microscopy with an x100
152 objective lens (Olympus, Tokyo, Japan).

153 **Measurements Inflammatory Mediators and cell death marker**

154 The levels of IL-1ß, TNF-α, IL-6, IL-8 and LDH were quantified in the culture
155 supernatants from infected and uninfected monocytes using ELISA kits, according to the
156 manufacturer's intructions (R&D System).

157 Extracellular lactate dehydrogenase (LDH) was quantified using Doles® kit
158 according to manufacturer's instructions. In brief, cell culture supernatants were
159 centrifuged at 5,000 rpm for 1 minute, to remove cellular debris, and then 25 µL were
160 placed into 96-well plates and incubated with 5 µL of ferric alum and 100 µL of LDH
161 substrate for 3 minutes at 37 ºC. Nicotinamide adenine dinucleotide (NAD, oxidized
162 form) was added followed by the addition of a stabilizing solution. After 10 minutes, the
163 reaction was read in a spectrophotometer at 492 nm.

164 **Western blot assay**

165 Cellular extracts of $1x10^6$ cells were homogenized in the RIPA lysis buffer in the
166 presence of proteinase inhibitor cocktail (Roche), and the protein levels were measured
167 by BCA protein assay kit. A total of 20 µg of protein was loaded onto a 10% sodium
168 dodecyl sulfate polyacrylamide gel (SDS-PAGE) for separation by electrophoresis and
169 the protein bands were then transferred to a polyvinylidene difluoride membranes
170 (ImmobilonP-SQ, Millipore). The membranes were blocked with 5 % albumin diluted in
171 Tris-buffered saline containing 0.05 % of Tween 20 for 2 hours at room temperature and
172 incubated with the specific primary antibodies (Cell Signaling Technology), to detect pro-
173 caspase-1 and cleaved-caspase-1, after overnight incubation at 4 °C. After washing,
174 membranes were incubated with secondary antibodies (IRDye® 800CW Goat-anti-
175 Mouse and IRDye® 680LT Goat anti-Rabbit IgG Antibody, LI-COR, Lincoln) for 30
176 minutes at RT. The protein bands were visualized by digital fluorescence
177 (Odyssey® CLx Imaging System), and protein density was analyzed by the ImageJ
178 software. All the data were normalized by β-actin expression quantification.

179

180

181 **Human subjects.**

182 We prospectively enrolled severe COVID19 RT-PCR-confirmed cases, as well as
183 SARS-CoV-2-negative healthy controls. Blood samples were obtained from 12 patients
184 with severe COVID-19 within 72 hours from intensive care unit (ICU) admission in two
185 reference centers (Instituto Estadual do Cérebro Paulo Niemeyer and Hospital Copa Star,
186 Rio de Janeiro, Brazil). Severe COVID-19 was defined as critically ill patients presenting
187 viral pneumonia on computed tomography scan and in mechanical ventilation. All
188 patients had SARSCoV-2 confirmed diagnostic through RT-PCR of nasal swab or
189 tracheal aspirates. Peripheral vein blood was also collected from 8 SARS-CoV-2-negative
190 healthy control participants as tested by RT-PCR on the day of blood sampling. The
191 characteristics of severe (n = 12), and control (n = 8) participants are presented in Table
192 1. Severe COVID-19 patients usually present older age and higher prevalence of
193 comorbidities as obesity, cardiovascular diseases and diabetes as in previously reported
194 patient cohorts. In the present study, the SARS-CoV-2-negative control group was
195 designed to include subjects of older age and chronic non-communicable diseases, so it
196 is matched with critically ill COVID-19 patients (Table 1). Patients with acute respiratory
197 distress syndrome (ARDS) were managed with neuromuscular blockade and a protective
198 ventilation strategy that included low tidal volume (6 mL/kg of predicted body weight)
199 and limited driving pressure (less than 16 cmH2O) as well as optimal PEEP calculated
200 based on the best lung compliance and PaO_2/FiO_2 ratio. In those with severe ARDS and
201 PaO_2/FiO_2 ratio below 150 despite optimal ventilatory settings, prone position was
202 initiated. Our management protocol included antithrombotic prophylaxis with enoxaparin
203 40 to 60 mg per day. Patients did not receive routine steroids, antivirals or other anti-
204 inflammatory or anti-platelet drugs. The SARS-CoV-2- negative control participants
205 were not under anti-inflammatory or anti-platelet drugs for at least two weeks. All clinical
206 information were prospectively collected using a standardized form - ISARIC/WHO
207 Clinical Characterization Protocol for Severe Emerging Infections (CCPBR).

208 **Ethics statement.**

209 Experimental procedures involving human cells from healthy donors were
210 performed with samples obtained after written informed consent and were approved by
211 the Institutional Review Board (IRB) of the Oswaldo Cruz Foundation/Fiocruz (Rio de
212 Janeiro, RJ, Brazil) under the number 397-07. The National Review Board approved the

213 study protocol (CONEP 30650420.4.1001.0008), and informed consent was obtained
214 from all participants or patients' representatives.

215 **Statistical analysis**

216 The assays were performed in blinded way. They were performed by one
217 professional, codified and read by another fellow. All experiments were carried out at
218 least three independent times, including a minimum of two technical replicates in each
219 assay. The dose-response curves used to calculate EC50 and CC50 values were generated
220 by variable slope plot from Prism GraphPad software 8.0. The equations to fit the best
221 curve were generated based on R^2 values ≥ 0.9. Student's T-test was used to access
222 statistically significant P values <0.05. The statistical analyses specific to each software
223 program used in the bioinformatics analysis are described above.

224 ## Results

225 **SARS-CoV-2 promotes pyroptosis in human monocytes**

226 To explore the mechanism by which SARS-CoV-2 triggers monocyte death,
227 human primary monocytes were infected and treated with pharmacological inhibitors of
228 pyroptosis (AC-YVAD-CMK, an inhibitor of Caspase-1 activity), apoptosis (ZVAD-
229 FMK, a pan-caspase inhibitor), and necroptosis (Nec-1, an inhibitor of Receptor-
230 interacting serine/threonine-protein kinase 1; RIPK1). Next, cell death was analyzed by
231 quantifying the LDH activity in the culture supernatant, and by AnnexinV/propidium
232 iodide (PI) cell labeling through for flow cytometry and fluorescence microscopy. As
233 shown in Figure 1A, SARS-CoV-2 increased LDH levels similarly to the positive control,
234 LPS+ATP (Figure 1A). Whereas AC-YVAD-CMK prevented SARS-COV-2-induced
235 cell death, ZVAD-FMK and Nec-1 did not affect SARS-CoV-2-induced LDH release
236 (Figure 1A). Flow cytometry and fluorescence microscopy images demonstrated higher
237 percentages of PI^+ cells in the infected cultures, as well as a significant increase in mean
238 fluorescence intensity (MFI). Both, LDH leak and PI labeling characterize cell membrane
239 disruption in human monocytes after SARS-CoV-2 infection (Figure 1B-D). SARS-CoV-
240 2-induced PI positivity was also prevented by AC-YVAD-CMK treatment (Figure 1B -
241 D). These data suggest that SARS-CoV-2 infection can induce pyroptosis.

242 **SARS-CoV-2 induces pyroptosis in monocytes through inflammasome activation**

243 To gain insights on the mechanisms of monocyte pyroptosis in SARS-CoV-2
244 infection, we accessed caspase-1 and IL-1 activation - two key events that require
245 inflammasome's proteolytic activity. To do so, human monocytes were pretreated with
246 AC-YVAD-CMK or the IL-1 receptor antagonist (IL-1RA), and infected with SARS-
247 CoV-2. Cells stimulated with LPS+ATP were used as a positive control of inflammasome
248 activation. We observed that SARS-CoV-2 induced pro-caspase-1 cleavage, similarly to
249 positive control (Figure 2A). Caspase-1 activation was not observed in infected cells
250 pretreated with AC-YVAD-CMK (Figure 2A). To confirm these results, cells were
251 labeled with FAM-YVAD-FLICA (as an indicative of caspase-1 activation) and analyzed
252 by flow cytometry. We found that SARS-CoV-2 infection induced the activation of
253 caspase-1 in monocytes in the same magnitude to the positive control group (Figure 2B).
254 Moreover, SARS-CoV-2-induced caspase-1 activation was a specific event, since we did
255 not observe activation of the apoptotic caspases-3 and -7 in infected monocytes (Figure
256 2C). Importantly, inhibition of IL-1R engagement reduced SARS-CoV-2-mediated
257 caspase-1 activation and LDH release, suggesting that inflammasome-dependent IL-1β
258 secretion amplify caspase-1 activation and pyroptosis in SARS-CoV-2 infection (Figure
259 2B and 2D).

260 **Inflammasome activation amplify pro-inflammatory cytokines secretion in infected**
261 **monocytes**

262 As caspase-1 activity is critical for the production of IL-1β (15,16), we measured
263 the levels of this cytokine in our experiments. Our data show that SARS-CoV-2 infection
264 was able to increase IL-1β production (Figure 2A). This increment was prevented by the
265 treatment with caspase-1 pharmacological inhibitor AC-YVAD-CMK and the pan-
266 caspase inhibitor ZVAD (Figure 2A). To confirm whether the observed effect is
267 specifically related to inflammasome activation, we evaluated the production of IL-8, in
268 which induction is independent of the inflammasomes pathway. SARS-CoV-2 infection
269 induced a higher IL-8 production, which was not prevented by caspase-1 inhibition
270 (Figure 2B). Importantly, caspase-1 specific inhibition, but not pan-caspase or RIPK1
271 inhibitor, also led to lower levels of the pro-inflammatory cytokines IL-6 and TNF-α,
272 highlighting the participation of the caspase-1-IL-1β axis in inflammatory amplification
273 during SARS-CoV-2 infection. (Figure 3C and 3D).

274 **Infection with SARS-CoV-2 decreases the expression of HLA class II in human**
275 **monocytes independently of the activation of inflammasomes**

276 To investigate the impact of inflammasome activation and cell death through
277 pyroptosis on the orchestration of anti-SARS-CoV-2 immune response, human
278 monocytes were pretreated with AC-YVAD-CMK or with IL-1RA, and then infected
279 with SARS-CoV-2. Cells were then marked with HLA-DR and analyzed by flow
280 cytometry. We found that SARS-CoV-2 infection induced a decrease in HLA-DR
281 expression in monocytes (Figure 3A and B). However, the inhibition of caspase-1 and
282 IL-1R engagement did not prevent the SARS-CoV-2-mediated decreasing of HLA
283 expression (Figure 3C and D).

284 **Atazanavir prevented inflammasome-dependent pyroptosis**

285 Given our findings that pyroptosis and decreased HLA-DR expression are
286 triggered during SARS-CoV-2 replication, we tested whether atazanavir (ATV), an HIV
287 protease inhibitor recently shown to possess antiviral activity against the new CoV in
288 monocytes (17), could prevent these events. Flow cytometry analysis of SARS-CoV-2-
289 infected monocytes treated with ATV demonstrated a significant reduction in caspase-1
290 activity, observed by the decreased FAM-YVAD-FLICA labeling (Figure 4A). Other
291 orally available repurposed anti-SARS-CoV-2 drugs, such as lopinavir (LPV) and
292 ribavirin (RBV), did not affect SARS-CoV-2-induced pyroptosis (Figure 4B). Moreover,
293 treatments with ATV did not alter the activity of caspase-1, -3 and -7 in monocytes
294 exposed to LPS and ATP, used as a positive control of pyroptosis (Figure S2), indicating
295 a specific antiviral activity of this drug. Consistently, treatment with ATV also reduced
296 the levels of IL-1β, IL-6 and TNF-α in SARS-CoV-2-infected monocytes, when
297 compared to the untreated cells (Figure 4C-F). ATV did not interfere with the production
298 of IL-8, which is independent of inflammasome engagement (Figure 4D).

299 We then confirmed whether ATV can prevent SARS-CoV-2-induced pyroptosis.
300 Lower levels of LDH were detected in the supernatants of SARS-CoV-2-infected
301 monocytes treated with ATV when compared to infected and untreated cells (Figure 4G).
302 The treatment with ATV was also able to prevent the decrease of HLA-DR expression in
303 infected monocytes (Figure 4H and I). LPV and RBV did not alter the HLA expression
304 in monocytes infected with SARS-Cov-2 (Figure S3).

305 **Inflammasome activation and pyroptosis are risk factors in critically ill COVID-19**
306 **patients**

307 To clinically validate our findings, we evaluated if monocytes obtained from
308 critically ill patients with COVID-19 would also display signals of inflammasome
309 engagement and pyroptosis. Western blot analyzes showed that monocytes from
310 COVID-19 patients had increased levels of cleaved caspase-1 compared to monocytes
311 from healthy donors (HD) (Figure 5A). To confirm this result, cells were marked with
312 FAM-YVAD-FLICA and analyzed by flow cytometry. We observed that monocytes from
313 COVID-19 patients had increased caspase-1 activation (Figure 5B) and significantly
314 higher PI+ staining, when compared to monocytes from HD (Figure 5C). Corroborating
315 with our *in vitro* data, we also detected higher levels of IL-1β in the plasma of critically
316 ill patients (Figure 5D).

317 **SARS-CoV-2 infection induces inflammasome-dependent pyroptosis and**
318 **downmodulation of HLA-DR monocytes, which can be prevented by atazanavir**

319 Representative scheme demonstrating the effect of SARS-CoV-2 infection by
320 stimulating the production of TNF-alpha and IL-6 and by another way promoting the
321 assembly of inflammasomes leading to activation of caspase-1 and release of cleaved IL-
322 1ß and pyroptosis cell death. Release of IL-1ß amplify the activation of inflammasomes
323 during the SARS-CoV-2 infection. SARS-CoV-2 also induces the HLA-DR
324 downregulation independently of the activation of inflammasomes and ATV treatment
325 prevents the formation of inflammasomes with the consequent release of IL-1ß, and also
326 preserves the expression of HLA-DR in the treated human monocytes.

327 ## Discussion

328 COVID-19 has caused in less than 8 months over 800,000 deaths worldwide (18)
329 and represent the major public health crisis of the beginning of 21st century, leading to an
330 unimaginable impact in global economics (19,20). SARS-CoV-2 infection triggers an
331 uncontrolled inflammatory response and marked leukopenia with consequent
332 lung/respiratory dysfunction, which are the characteristics of the most severe
333 manifestations of the COVID-19 (21,22). Similarly to other respiratory viruses (23-25),
334 SARS-CoV-2 induces a cytokine storm, characterized by an uncontrolled inflammatory

335 response mediated by monocytes/macrophages, when they should orchestrate the
336 antiviral immune response (26,27). In this work, we demonstrate that SARS-CoV-2
337 infection triggers inflammasome activation, increases IL-1ß secretion by monocytes,
338 resulting in pyroptotic cell death, which could be a key event for SARS-CoV-2
339 pathogenesis in critically ill patients and prevented by antiviral drugs (28).

340 Our results demonstrate that SARS-CoV-2 leads to an intense cell death in human
341 monocytes, observed by the increase in LDH release in infected cultures as well as by the
342 higher number of PI^+ cells when compared to uninfected controls. Even though the
343 pretreatment of infected monocytes with the pan-caspase inhibitor ZVAD-FMK
344 prevented IL-1β secretion, it was not able to prevent the release of LDH. Indeed, others
345 have demonstrated that the treatment with ZVAD-FMK induces necroptosis in diverse
346 cell types (29-31). Notably, as pyroptosis is an inflammatory and programmed cell death
347 mediated by inflammasome and inflammatory caspase-1 activation (13,14), we
348 investigated the assembly and activation of these structures in human monocytes infected
349 with SARS-CoV-2. Activation of caspase-1 and increased production of IL-1ß were
350 observed in infected monocytes. This is correlated to the activation of inflammasomes,
351 because the pretreatment of infected monocytes with YVAD inhibited the activation of
352 caspase-1. These results are in accordance with the literature that suggests the formation
353 of inflammasomes in patients with severe COVID-19 (21). We also showed that the
354 release of IL-1ß could be promoted by and at the same time amplify the activation of
355 inflammasomes during the SARS-CoV-2 infection, since the blockage of IL-1ß receptors
356 reduced caspase-1 activation and cell death. This result corroborates with studies showing
357 that the increase in IL-1ß production is associated with severe COVID-19 (32-34). Under
358 our experimental conditions, the increase in IL-1ß precedes the unbalanced IL-6 release.

359 Monocytes that survived from SARS-CoV-2 infection displayed decreased HLA-
360 DR expression, which has also been described in monocytes isolated from COVID-19
361 patients (35,36). Our results suggest that this modulation of HLA expression is not
362 directly associated with the activation of inflammasomes, and may be involved by other
363 inflammatory pathways, since we and other have observed increased levels of IL-6 by
364 myeloid cells impairing HLA-DR membrane expression (37).

365 To correlate the phenomena of pyroptosis induction and inflammasome activation
366 observed in our *in vitro* studies with clinical reports in the literature (38,39), we analyzed

367 peripheral monocytes isolated from patients with severe COVID-19. We found that these
368 cells present higher caspase-1 activation when compared with monocytes isolated from
369 HD. Recent clinical data reports reveal the presence of high levels of LDH and leukopenia
370 in critically ill patients (6,8,40,41). Our data also demonstrate intense monocyte death in
371 COVID-19 patients as detected through flow cytometry analyzes. Altogether, these data
372 suggest that the severity of COVID-19 may be associated with inflammasome activation
373 in monocytes that results in large amounts of IL-1ß and generates an excessive
374 inflammatory response characterized by high levels of IL-6 and TNF-α. Consistently,
375 treatment with IL-1RA has been associated with clinical and inflammatory improvements
376 in critically ill COVID-19 patients (42). These results are in line with clinical case reports
377 that demonstrate that monocytes/macrophages are key cells in the deleterious pro-
378 inflammatory events that characterize the most serious cases of COVID-19 (43-46).

379 Effective therapies for COVID-19 should combine antiviral with anti-
380 inflammatory properties to reduce viral load and to mitigate the intense inflammatory
381 response. In the present study we used ATV, an antiretroviral approved in 2003 for HIV-
382 1 treatment and previously described by us as having anti-SARS-CoV-2 effects in
383 different cell types (including monocytes) and impairing virus-induced enhancement of
384 IL-6 and TNF-α levels (17). Our data reveal that ATV, besides inhibiting inflammasome
385 and pyroptosis, prevents the decreasing of HLA expression in monocytes infected with
386 SARS-CoV-2. In addition, ATV inhibited the release of LDH and the production of IL-
387 1ß, f IL-6 and TNF-α by SARS-CoV-2-infected monocytes, which are key players in the
388 cytokine storm associated with COVID-19 (47,48).

389 In this work, we originally describe that infection with SARS-CoV-2 can induce
390 pyroptotic cell death by inflammasome activation, which may be related to the intense
391 leukopenia and exacerbated inflammation seen in severe cases of the COVID-19. Since
392 there is no specific therapy for this disease, our results point out that ATV has a promising
393 therapeutic potential against SARS-CoV-2-induced cell death.

394 **Acknowledgments and funding**

395 We thank the Hemotherapy Service from Hospital Clementino Fraga Filho
396 (Federal University of Rio de Janeiro, Brazil) for providing buffy-coats. This work was
397 supported by grants from Fundação de Amparo a Pesquisa do Estado do Rio de Janeiro

(FAPERJ), Inova Fiocruz, Conselho Nacional de Desenvolvimento Científico e Tecnológico (CNPq) and Coordenação de Aperfeiçoamento de Pessoal de Nível Superior (CAPES) and Mercosur Fund for Structural Convergence (FOCEM, Mercosur, grant number 03/11) granted for Thiago Moreno L. Souza, Patrícia T. Bozza, Fernando A. Bozza and Dumith Chequer Bou-Habib. Funding was also provided by CNPq, CAPES and FAPERJ through the National Institutes of Science and Technology Program (INCT) to Carlos Morel (INCT-IDPN) and to Wilson Savino (INCT-NIM). Thanks are due to Oswaldo Cruz Foundation/Fiocruz under the auspicious of Inova program. The funding sponsors had no role in the design of the study; in the collection, analyses, or interpretation of data; in the writing of the manuscript, and in the decision to publish the results.

References

1. Conti P, Ronconi G, Caraffa A, Gallenga CE, Ross R, Frydas I, et al. Induction of pro-inflammatory cytokines (IL-1 and IL-6) and lung inflammation by COVID-19: anti-inflammatory strategies. Journal of biological regulators and homeostatic agents. 2020.

2. Long B, Brady WJ, Koyfman A, Gottlieb M. Cardiovascular complications in COVID-19. American Journal of Emergency Medicine. 2020.

3. Li J, Fan J-G. Characteristics and Mechanism of Liver Injury in 2019 Coronavirus Disease. J Clin Transl Hepatol. 2020.

4. Giamarellos-Bourboulis EJ, Netea MG, Rovina N, Akinosoglou K, Antoniadou A, Antonakos N, et al. Complex Immune Dysregulation in COVID-19 Patients with Severe Respiratory Failure. Cell Host Microbe. 2020.

5. Du RH, Liang LR, Yang CQ, Wang W, Cao TZ, Li M, et al. Predictors of mortality for patients with COVID-19 pneumonia caused by SARSCoV- 2: A prospective cohort study. Eur Respir J. 2020.

6. Zhou F, Yu T, Du R, Fan G, Liu Y, Liu Z, et al. Clinical course and risk factors for mortality of adult inpatients with COVID-19 in Wuhan, China: a retrospective cohort study. Lancet. 2020.

427 7. Wölfel R, Corman VM, Guggemos W, Seilmaier M, Zange S, Müller MA, et al.
428 Virological assessment of hospitalized patients with COVID-2019. Nature. 2020.

429 8. Xu Z, Shi L, Wang Y, Zhang J, Huang L, Zhang C, et al. Pathological findings of
430 COVID-19 associated with acute respiratory distress syndrome. Lancet Respir
431 Med. 2020.

432 9. Han Y, Zhang H, Mu S, Wei W, Jin C, Xue Y, et al. Lactate dehydrogenase, a
433 Risk Factor of Severe COVID-19 Patients. medRxiv. 2020.

434 10. Terpos E, Ntanasis-Stathopoulos I, Elalamy I, Kastritis E, Sergentanis TN, Politou
435 M, et al. Hematological findings and complications of COVID-19. American
436 Journal of Hematology. 2020.

437 11. Li YX, Wu W, Yang T, Zhou W, Fu YM, Feng QM, et al. [Characteristics of
438 peripheral blood leukocyte differential counts in patients with COVID-19].
439 Zhonghua nei ke za zhi. 2020.

440 12. Ding X, Yu Y, Lu B, Huo J, Chen M, Kang Y, et al. Dynamic profile and clinical
441 implications of hematological parameters in hospitalized patients with
442 coronavirus disease 2019. Clin Chem Lab Med. 2020.

443 13. Singh A, Sood N, Narang V, Goyal A. Morphology of COVID-19-affected cells
444 in peripheral blood film. BMJ Case Reports. 2020.

445 14. Zalinger ZB, Elliott R, Weiss SR. Role of the inflammasome-related cytokines Il-
446 1 and Il-18 during infection with murine coronavirus. J Neurovirol. 2017.

447 15. Franchi L, Eigenbrod T, Muñoz-Planillo R, Nuñez G. The inflammasome: A
448 caspase-1-activation platform that regulates immune responses and disease
449 pathogenesis. Nature Immunology. 2009.

450 16. Miao EA, Rajan J V., Aderem A. Caspase-1-induced pyroptotic cell death.
451 Immunological Reviews. 2011.

452 17. Fintelman-Rodrigues N, Sacramento CQ, Lima CR, Silva FS da, Ferreira A,
453 Mattos M, et al. Atazanavir inhibits SARS-CoV-2 replication and pro-
454 inflammatory cytokine production. bioRxiv. 2020.

455 18. OPAS. COVID-19 (doença causada pelo novo coronavírus). Folha Inf. 2020.

456 19. Dong E, Du H, Gardner L. An interactive web-based dashboard to track COVID-
457 19 in real time. The Lancet Infectious Diseases. 2020.

458 20. Wissel BD, Van Camp PJ, Kouril M, Weis C, Glauser TA, White PS, et al. An
459 Interactive Online Dashboard for Tracking COVID-19 in U.S. Counties, Cities,
460 and States in Real Time. J Am Med Inform Assoc. 2020.

461 21. Lucas C, Wong P, Klein J, Castro TBR, Silva J, Sundaram M, et al. Longitudinal
462 analyses reveal immunological misfiring in severe COVID-19. Nature. 2020.

463 22. Tay MZ, Poh CM, Rénia L, MacAry PA, Ng LFP. The trinity of COVID-19:
464 immunity, inflammation and intervention. Nature Reviews Immunology. 2020.

465 23. Teijaro JR. The role of cytokine responses during influenza virus pathogenesis
466 and potential therapeutic options. Curr Top Microbiol Immunol. 2014.

467 24. Szretter KJ, Gangappa S, Lu X, Smith C, Shieh W-J, Zaki SR, et al. Role of Host
468 Cytokine Responses in the Pathogenesis of Avian H5N1 Influenza Viruses in
469 Mice. J Virol. 2007.

470 25. Peschke T, Bender A, Nain M, Gemsa D. Role of Macrophage Cytokines in
471 Influenza A Virus lnfections. Immunobiology. 1993.

472 26. Woo PCY, Tung ETK, Chan KH, Lau CCY, Lau SKP, Yuen KY. Cytokine
473 profiles induced by the novel swine-origin influenza A/H1N1 virus: Implications
474 for treatment strategies. J Infect Dis. 2010.

475 27. Jamilloux Y, Henry T, Belot A, Viel S, Fauter M, El Jammal T, et al. Should we
476 stimulate or suppress immune responses in COVID-19? Cytokine and anti-
477 cytokine interventions. Autoimmunity Reviews. 2020.

478 28. Zheng Z, Peng F, Xu B, Zhao J, Liu H, Peng J, et al. Risk factors of critical &
479 mortal COVID-19 cases: A systematic literature review and meta-analysis.
480 Journal of Infection. 2020.

481 29. Siegmund D, Kums J, Ehrenschwender M, Wajant H. Activation of TNFR2
482 sensitizes macrophages for TNFR1-mediated necroptosis. Cell Death Dis. 2016.

483 30. Kim SJ, Li J. Caspase blockade induces RIP3-mediated programmed necrosis in
484 Toll-like receptor-activated microglia. Cell Death Dis. 2013.

485 31. Wu YT, Tan HL, Huang Q, Sun XJ, Zhu X, Shen HM. ZVAD-induced necroptosis
486 in L929 cells depends on autocrine production of TNFα mediated by the PKC-
487 MAPKs-AP-1 pathway. Cell Death Differ. 2011.

488 32. Abbasifard M, Khorramdelazad H. The bio-mission of interleukin-6 in the
489 pathogenesis of COVID-19: A brief look at potential therapeutic tactics. Life
490 Sciences. 2020.

491 33. Yao Z, Zheng Z, Wu K, Zheng J. Immune environment modulation in pneumonia
492 patients caused by coronavirus: SARS-CoV, MERS-CoV and SARS-CoV-2.
493 Aging (Albany NY). 2020.

494 34. Zhang Y, Li J, Zhan Y, Wu L, Yu X, Zhang W, et al. Analysis of serum cytokines
495 in patients with severe acute respiratory syndrome. Infect Immun. 2004.

496 35. Ong EZ, Chan YFZ, Leong WY, Lee NMY, Kalimuddin S, Haja Mohideen SM,
497 et al. A Dynamic Immune Response Shapes COVID-19 Progression. Cell Host
498 Microbe. 2020.

499 36. Laing AG, Lorenc A, del Molino del Barrio I, Das A, Fish M, Monin L, et al. A
500 dynamic COVID-19 immune signature includes associations with poor prognosis.
501 Nat Med [Internet]. 2020; Available from: https://doi.org/10.1038/s41591-020-
502 1038-6.

503 37. Ohno Y, Kitamura H, Takahashi N, Ohtake J, Kaneumi S, Sumida K, et al. IL-6
504 down-regulates HLA class II expression and IL-12 production of human dendritic
505 cells to impair activation of antigen-specific CD4+ T cells. Cancer Immunol

506 Immunother. 2016.
507 38. Yap JKY, Moriyama M, Iwasaki A. Inflammasomes and Pyroptosis as Therapeutic
508 Targets for COVID-19. J Immunol. 2020.

509 39. Rodrigues S, de Sá KS, Ishimoto AY, Becerra A, Oliveira S, Almeida L, et al.
510 Inflammasome activation in COVID-19 patients 1 2 Tamara. medRxiv. 2020.
511
512 40. Yuan J, Zou R, Zeng L, Kou S, Lan J, Li X, et al. The correlation between viral
513 clearance and biochemical outcomes of 94 COVID-19 infected discharged
514 patients. Inflamm Res. 2020.

515 41. Yan L, Zhang HT, Goncalves J, Xiao Y, Wang M, Guo Y, et al. An interpretable
516 mortality prediction model for COVID-19 patients. Nat Mach Intell. 2020.

517 42. Cauchois R, Koubi M, Delarbre D, Manet C, Carvelli J, Blasco VB, et al. Early
518 IL-1 receptor blockade in severe inflammatory respiratory failure complicating
519 COVID-19. Proc Natl Acad Sci. 2020.

520 43. Qin C, Zhou L, Hu Z, Zhang S, Yang S, Tao Y, et al. Dysregulation of immune
521 response in patients with COVID-19 in Wuhan, China. Clin Infect Dis. 2020.

522 44. McGonagle D, Sharif K, O'Regan A, Bridgewood C. The Role of Cytokines
523 including Interleukin-6 in COVID-19 induced Pneumonia and Macrophage
524 Activation Syndrome-Like Disease. Autoimmunity Reviews. 2020.

525 45. Merad M, Martin JC. Pathological inflammation in patients with COVID-19: a key
526 role for monocytes and macrophages. Nature Reviews Immunology. 2020.

527 46. Park MD. Macrophages: a Trojan horse in COVID-19? Nat Rev Immunol. 2020.
528
529 47. Hantoushzadeh S, Norooznezhad AH. Possible Cause of Inflammatory Storm and
530 Septic Shock in Patients Diagnosed with (COVID-19). Arch Med Res. 2020.

531 48. Hantoushzadeh S, Norooznezhad AH. Inappropriate Antibiotic Consumption as a
532 Possible Cause of Inflammatory Storm and Septic Shock in Patients Diagnosed
533 with Coronavirus Disease 2019 (COVID-19). Arch Med Res. 2020.

534 **FIGURE LEGENDS**

535 **Figure 1. SARS-Cov-2 induces monocyte cell death through pyroptosis.** Human
536 monocytes were pretreated with caspase-1 inhibitor (AC-YVAD-CMK – 1 μM), pan-
537 caspase inhibitor (ZVAD-FMK - 10 μM) or necroptosis inhibitor (Nec-1 - 25 μM) for 1
538 h and infected with SARS-Cov-2 (MOI 0.1) for 24 h. As a positive control, monocytes
539 were stimulated with LPS (500ng/mL) for 23 h and after this time, incubated with ATP
540 (2 mM) for 1 h. **(A)** Cell viability was assessed through the measurement of LDH release
541 in the supernatant of monocytes. **(B, C)** Monocytes` monolayers were stained with
542 propidium iodide (PI) plus Annexin V and pyroptotic cell death were determine by flow
543 cytometer analysis and **(D)** labeled with DAPI to visualize the nuclei fluorescence
544 microscopy. Images and Graph data are representative of six independent experiments.
545 Data are presented as the mean ± SEM * $P < 0.05$ *versus* control group (MOCK); $^{\#}$ $P <$
546 0.05 *versus* infected and untreated group (Nil).

547 **Figure 2. SARS-CoV-2 induce inflammasome activation in human monocytes.**
548 Human monocytes were pretreated with caspase-1 inhibitor (AC-YVAD-CMK – 1 μM),
549 pan-caspase inhibitor (ZVAD-FMK - 10 μM), necroptosis inhibitor (Nec-1 - 25 μM) or
550 inhibitor of IL-1ß receptor (IL-1RA – 1 μM) for 1 h and infected with SARS-Cov-2 (MOI
551 0.1) for 24 h. Monocytes were stimulated with LPS (500ng/mL) for 23 h and after this
552 time were stimulated with ATP (2 mM) for 1 h as a positive control group for the
553 formation of inflammasomes and pyroptosis induction. **(A)** Monocytes` monolayers were
554 used for determination of the levels of pro-caspase-1 and cleaved caspase-1 by western
555 blot analysis. **(B, C)** Monocytes were stained with FAM-YVAD-FLICA and FAM-
556 FLICA to determine the caspase-1 and caspase-3/7 activity, respectively, by flow
557 cytometry. **(D)** Cell culture supernatants were collected for the measurement of the levels
558 of LDH **(F)**. Western blot, histogram and graph data are representative of six independent
559 experiments. Data are presented as the mean ± SEM $^{\#}$ $P < 0.05$ *versus* infected and
560 untreated group (Nil); * $P < 0.05$ *versus* positive control group (LPS+ATP).

561 **Figure 3. Inflammasome activation amplify pro-inflammatory cytokines secretion**
562 **in infected monocytes.** Human monocytes were pretreated with caspase-1 inhibitor (AC-
563 YVAD-CMK – 1 μM), pan-caspase inhibitor (ZVAD-FMK - 10 μM), necroptosis
564 inhibitor (Nec-1 - 25 μM). Monocytes were stimulated with LPS (500ng/mL) for 23 h
565 and after this time were stimulated with ATP (2 mM) for 1 h as a positive control group

566 for the formation of inflammasomes and pyroptosis induction. Cell culture supernatants
567 were collected for the measurement of the levels of **(A)** IL-1β, **(B)** IL-8, **(C)** IL-6 and **(D)**
568 TNF-α. Graphs data are representative of six independent experiments. Data are presented
569 as the mean ± SEM $^{\#}$ $P < 0.05$ *versus* infected and untreated group (Nil); * $P < 0.05$ *versus*
570 positive control group (LPS+ATP).

571 **Figure 4. Infection with SARS-CoV-2 decreases the expression of HLA in human**
572 **monocytes independently of the activation of inflammasomes.** Human monocytes
573 were pretreated with caspase-1 inhibitor (AC-YVAD-CMK – 1 μM) or inhibitor of IL-
574 1ß receptor (IL-1RA – 1 μM) for 1 h and infected with SARS-Cov-2 for 24 h. **(A, B)**
575 Monocytes were stained with HLA-DR APC.H7 or IgG APC.H7 to determine the HLA-
576 DR expression by flow cytometry. **(C, D)** mean fluorescence intensity (MFI) value for
577 each sample was represented in graphics. Histogram and graphs datas are representative
578 of two independent experiments. Data are presented as the mean ± SEM $^{\#}$ $P < 0.05$ *versus*
579 uninfected group (MOCK).

580 **Figure 5. Atazanavir prevented inflammasome-dependent pyroptosis**. Human
581 monocytes were infected with SARS-Cov-2 and treated with atazanavir – ATV (10 μM),
582 ribavirina (10 μM) or Lopinavir (10 μM) for 24 h. **(A, B)** Monocytes were stained with
583 FAM-YVAD-FLICA or FAM-FLICA and HLA-DR APC.H7 or IgG APC.H7 to
584 determine the caspase-1 and caspase-3/7 activity and HLA-DR expression, respectively
585 and analyzed by flow cytometry. **(C – F)** Culture supernatants were collected and the
586 levels of IL-1β, IL-8, IL-6 and TNF-α were determined by ELISA. **(G)** Assessment of
587 cell viability through the measurement of LDH release in the supernatant of monocytes.
588 Histogram and graphs datas are representative of six independent experiments. Data are
589 presented as the mean ± SEM * $P < 0.05$ *versus* control group (MOCK); $^{\#}$ $P < 0.05$ *versus*
590 only infected group (Nil).

591 **Figure 6. Inflammasome activation and pyroptosis are risk factors in critically ill**
592 **COVID-19 patients.** Monocytes isolated from blood samples of critically ill patients
593 with COVID-19 and healthy donors. **(A)** Monocytes` extracts were used for to determine
594 the levels of pro-caspase-1 and cleaved caspase-1 and IL-1β by western blot analysis. In
595 addition, **(B and C, respectively)** monocytes were stained with FAM-YVAD-FLICA or
596 propidium iodide (PI) and analyzed by flow cytometry. **(D)** plasma was separated and the
597 levels of IL-1β were determined by ELISA. Western blot, histogram and graphs datas are

598 representative of 9 critically ill patients and 8 healthy donors. Data are presented as the
599 mean ± SEM * $P < 0.05$ *versus* healthy donors (HD).

600 **Figure 7.** Representative scheme of the SARS-CoV-2 infection in activation of
601 inflammasome and pyroptosis in monocyte with downregulation of HLA-DR expression
602 and effects of ATV treatment in this phenomenon.

603

604

605

606

607

608

609

610

611

612

613

614

615

616

617

618

619

620 **Table 1:** Characteristics of COVID-19 patients and control subjects.

621

Characteristics[1]	Control (N=8)	Covid-19 (N=9)
Age, years	52.6 (47 – 60)	61 (33 – 79)
Sex, male	8 (100 %)	6 (66.7 %)
Respiratory support		
Oxygen supplementation	0 (0 %)	3 (33.3 %)
Mechanical ventilation	0 (0 %)	6 (66.7 %)
SAPS 3		59.25 (31 – 75)
PaO2/FiO2 ratio	-	210.75 (87 – 509.5)
Vasopressor	-	3 (33.3 %)
Time from symptom onset to blood sample, days	-	10 (6 – 18)
Status on Jun 30th		
Dead	-	5 (55.55 %)
Discharged	-	1 (11.1 %)
Hospitalized	-	3 (33.3 %)
Comorbidities		
Obesity	1 (11.1 %)	1 (11.1 %)
Hypertension	3 (33.3%)	3 (33.3 %)
Diabetes	0 (0%)	0 (0 %)
Cancer	0 (0%)	0 (0 %)
Chronic heart disease[2]	0 (0%)	0 (0 %)
Presenting symptoms		
Cough	0 (0 %)	3 (33,3 %)
Fever	0 (0 %)	3 (33,3 %)
Dyspnea	0 (0 %)	4 (44,4 %)
Headache	0 (0 %)	0 (0 %)
Anosmia	0 (0 %)	0 (0 %)
Laboratory findings on admission		
Lymphocyte count, cells/mm^3	-	1,355.8 (552 –2,564)
Platelet count, x 1000/mm^3	-	169.6 (92 – 278)
Leukocytes	-	8,036 (8.03-18,670)
C Reactive Protein, mg/L	-	14.78 (0.1 – 30.8)

622 623 624 625 626 627 628 629 630 631 632 633 634 635 636 637 638 639 640 641 642 643 644 645 646

647

648

FIGURE 1

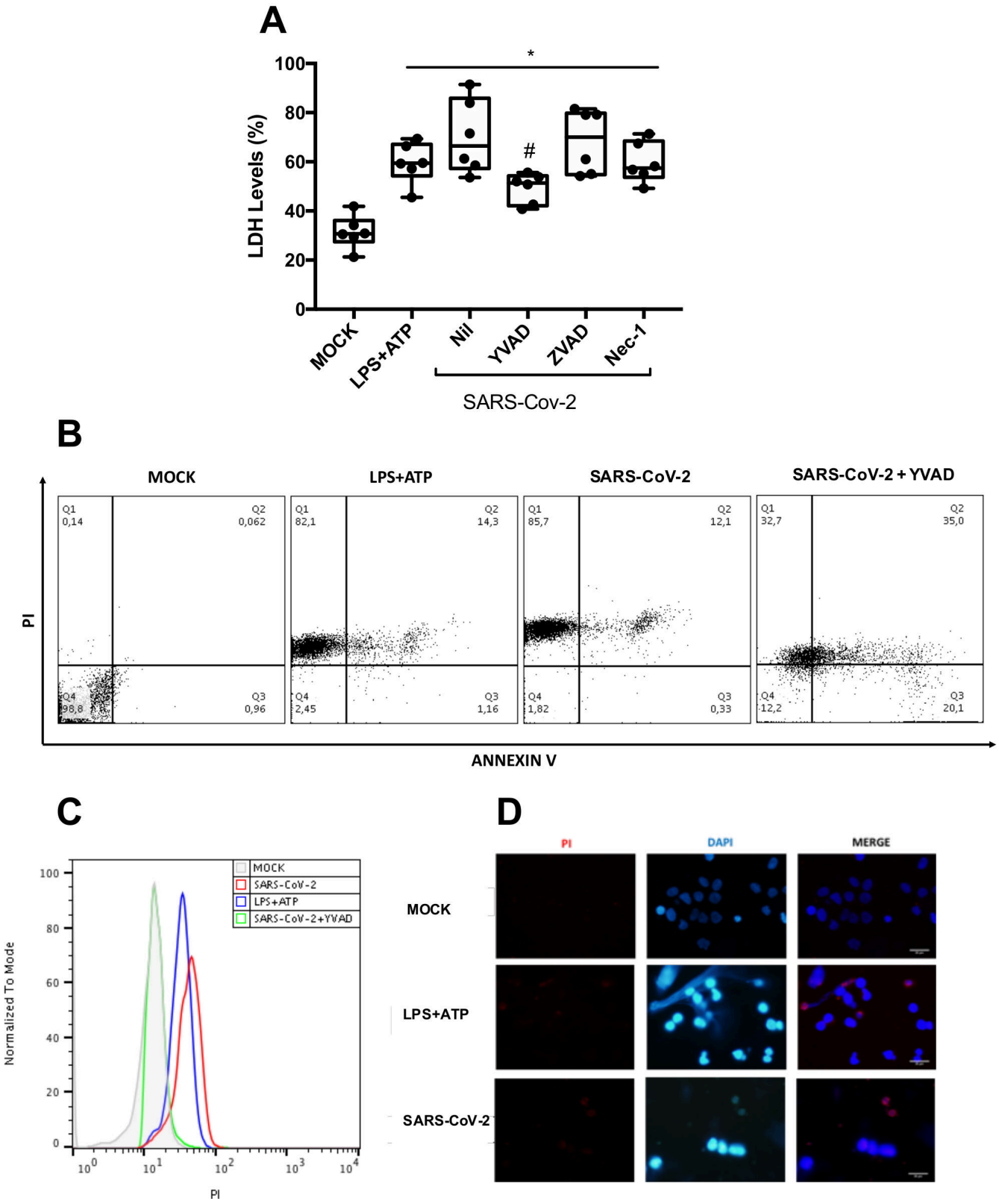
A
LDH Levels (%)
100
80
60
40
20
0
*
#
MOCK
LPS+ATP
Nil
YVAD
ZVAD
Nec-1
SARS-Cov-2
B
MOCK
LPS+ATP
SARS-CoV-2
SARS-CoV-2 + YVAD
PI
ANNEXIN V
Q1 0,14
Q2 0,062
Q4 98,8
Q3 0,96
Q1 82,1
Q2 14,3
Q4 2,45
Q3 1,16
Q1 85,7
Q2 12,1
Q4 1,82
Q3 0,33
Q1 32,7
Q2 35,0
Q4 12,2
Q3 20,1
C
MOCK
SARS-CoV-2
LPS+ATP
SARS-CoV-2+YVAD
Normalized To Mode
PI
D
PI
DAPI
MERGE
MOCK
LPS+ATP
SARS-CoV-2

683
684 **FIGURE 2**
685
686
687
688
689
690
691
692
693
694
695
696
697
698
699
700
701
702
703
704
705
706
707
708
709
710
711
712
713
714
715
716

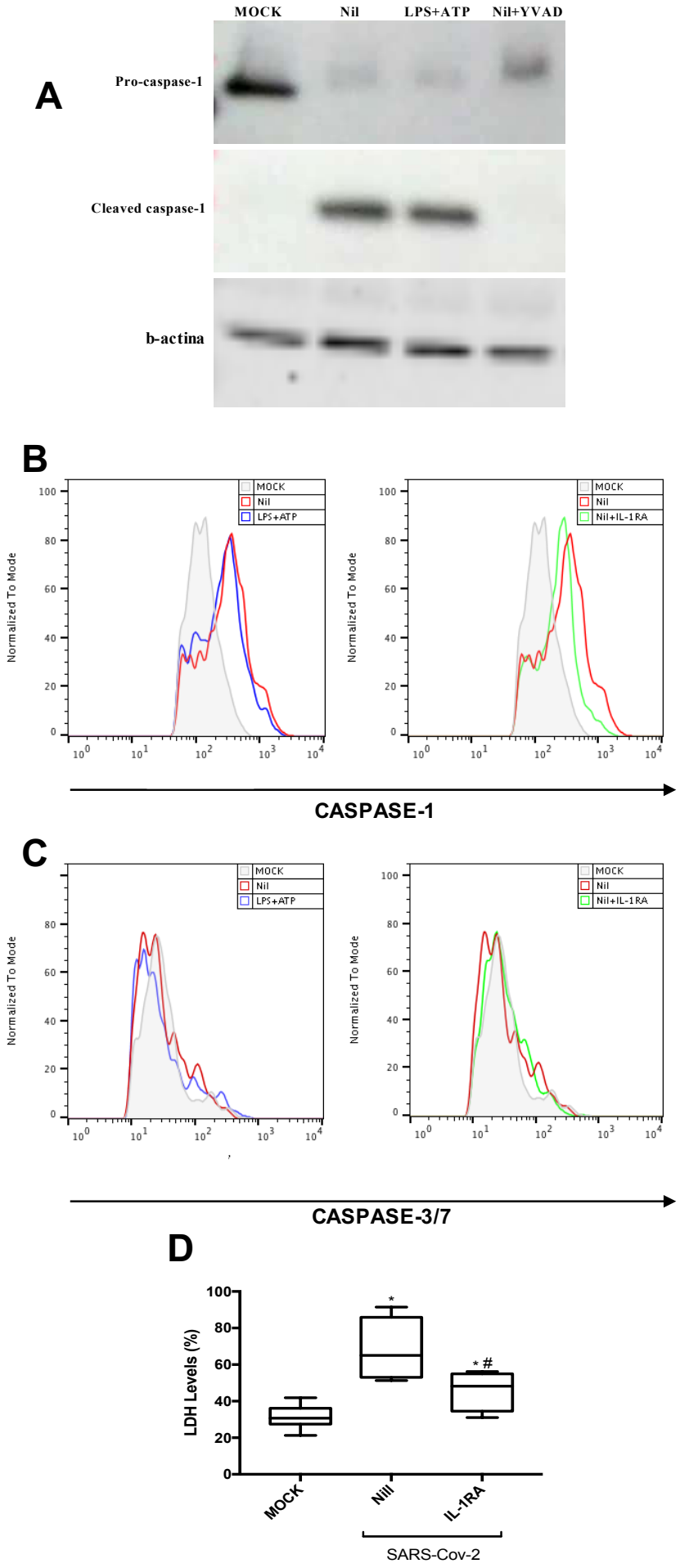

FIGURE 3

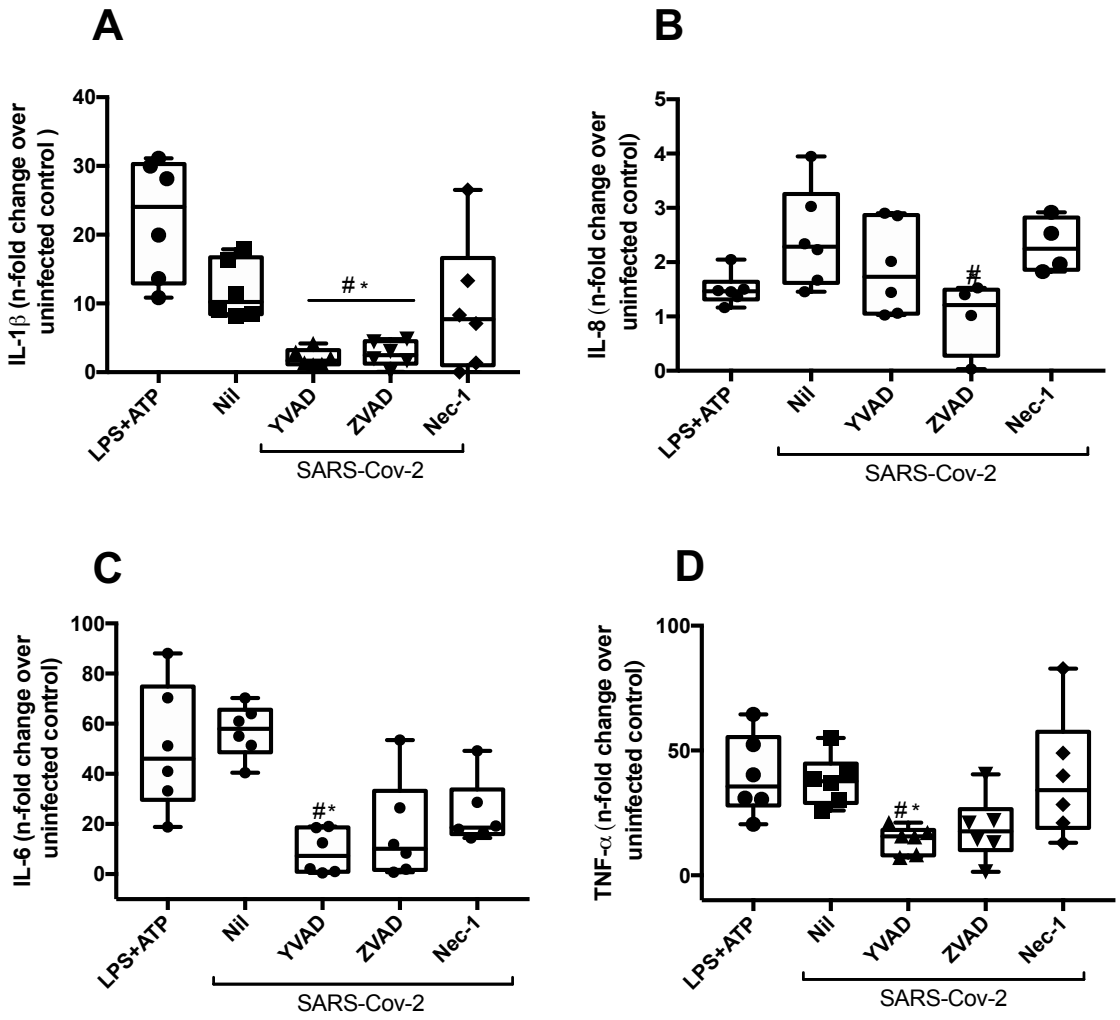
A
IL-1β (n-fold change over uninfected control)
40
30
20
10
0
#*
LPS+ATP
Nil
YVAD
ZVAD
Nec-1
SARS-Cov-2
B
IL-8 (n-fold change over uninfected control)
5
4
3
2
1
0
#
LPS+ATP
Nil
YVAD
ZVAD
Nec-1
SARS-Cov-2
C
IL-6 (n-fold change over uninfected control)
100
80
60
40
20
0
#*
LPS+ATP
Nil
YVAD
ZVAD
Nec-1
SARS-Cov-2
D
TNF-α (n-fold change over uninfected control)
100
50
0
#*
LPS+ATP
Nil
YVAD
ZVAD
Nec-1
SARS-Cov-2

FIGURE 4

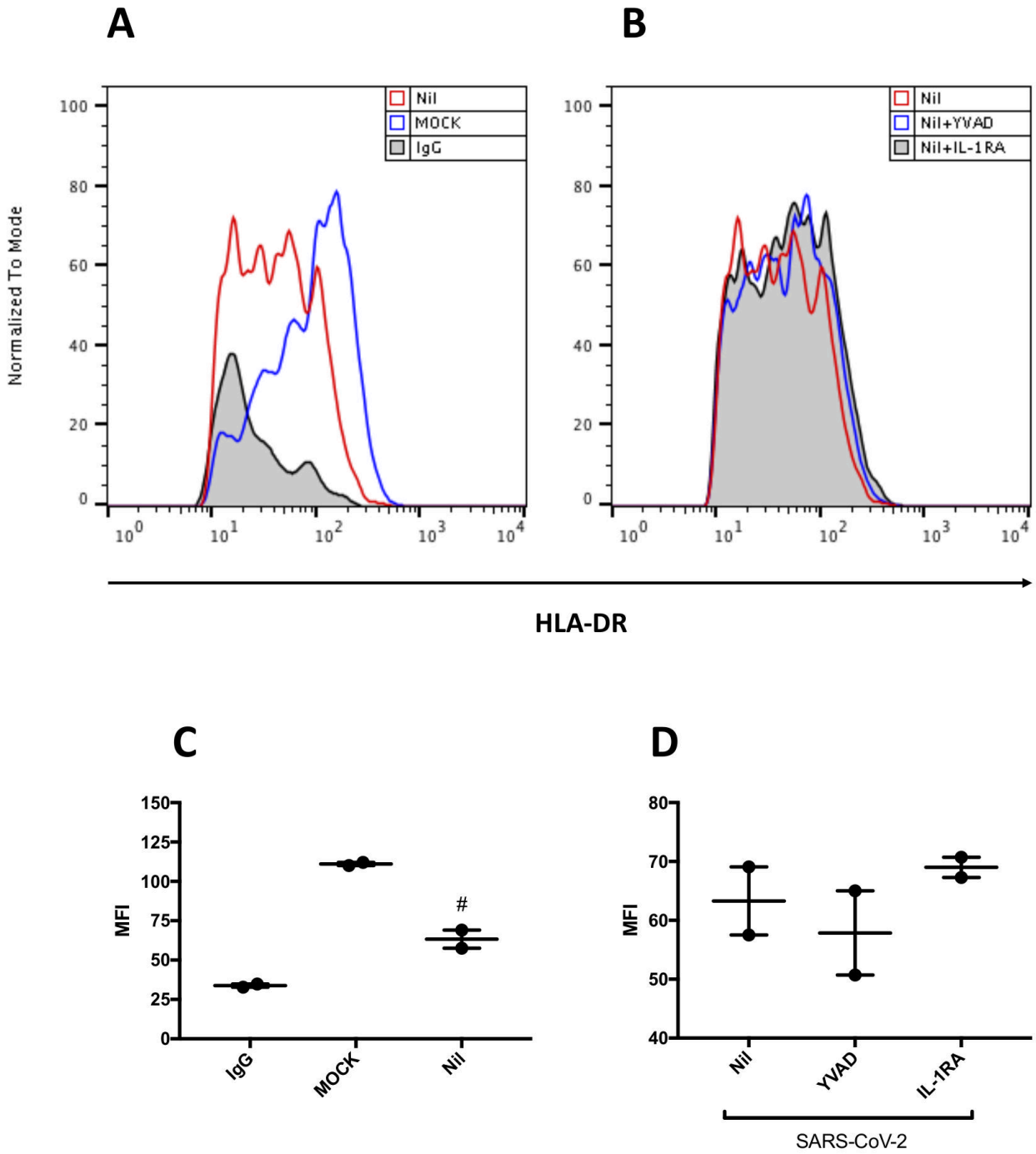
A
B
Nil
MOCK
IgG
Nil+YVAD
Nil+IL-1RA
Normalized To Mode
HLA-DR
C
D
MFI
#
IgG
MOCK
Nil
YVAD
IL-1RA
SARS-CoV-2

785 **FIGURE 5**

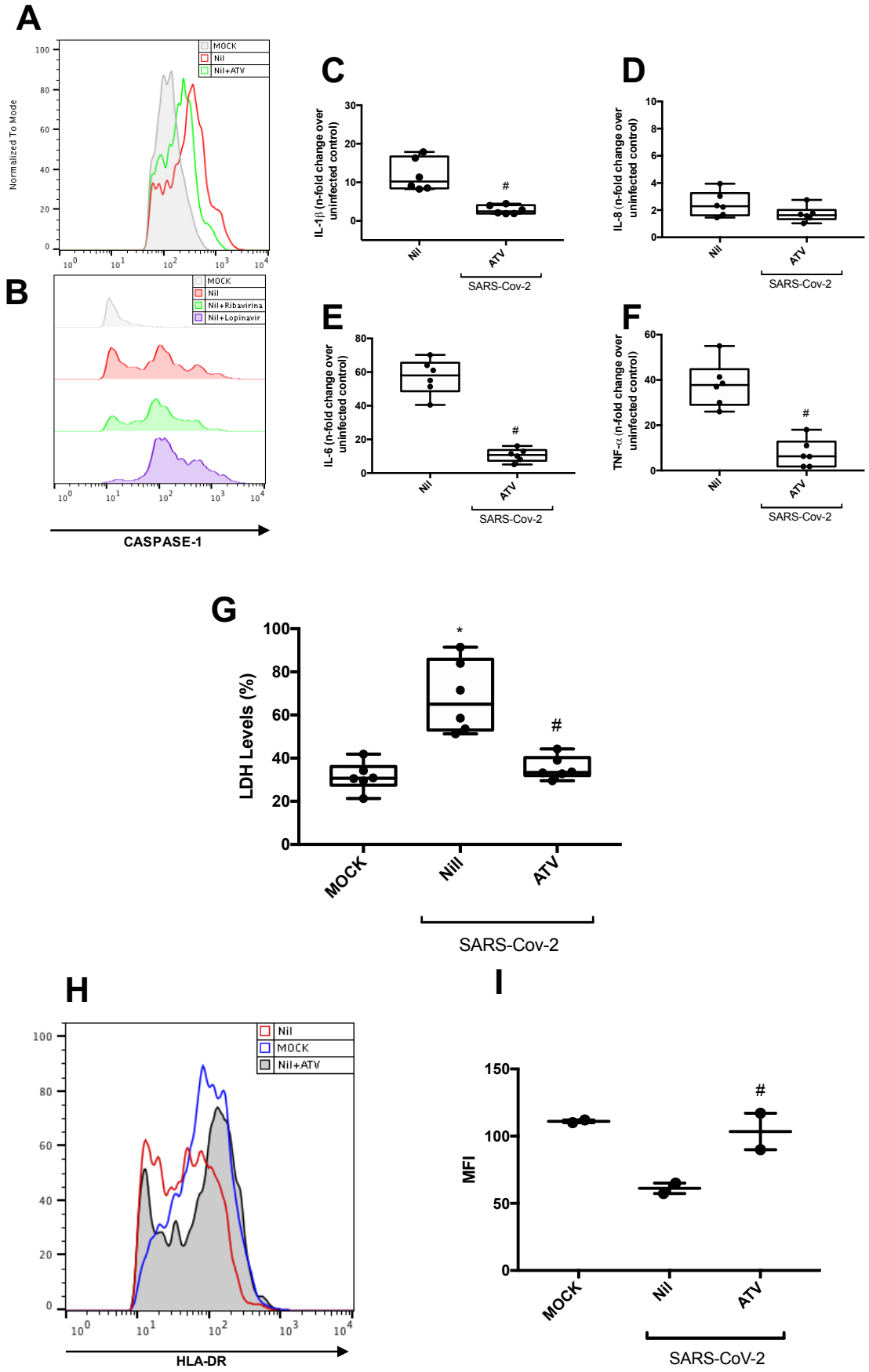

786

FIGURE 6

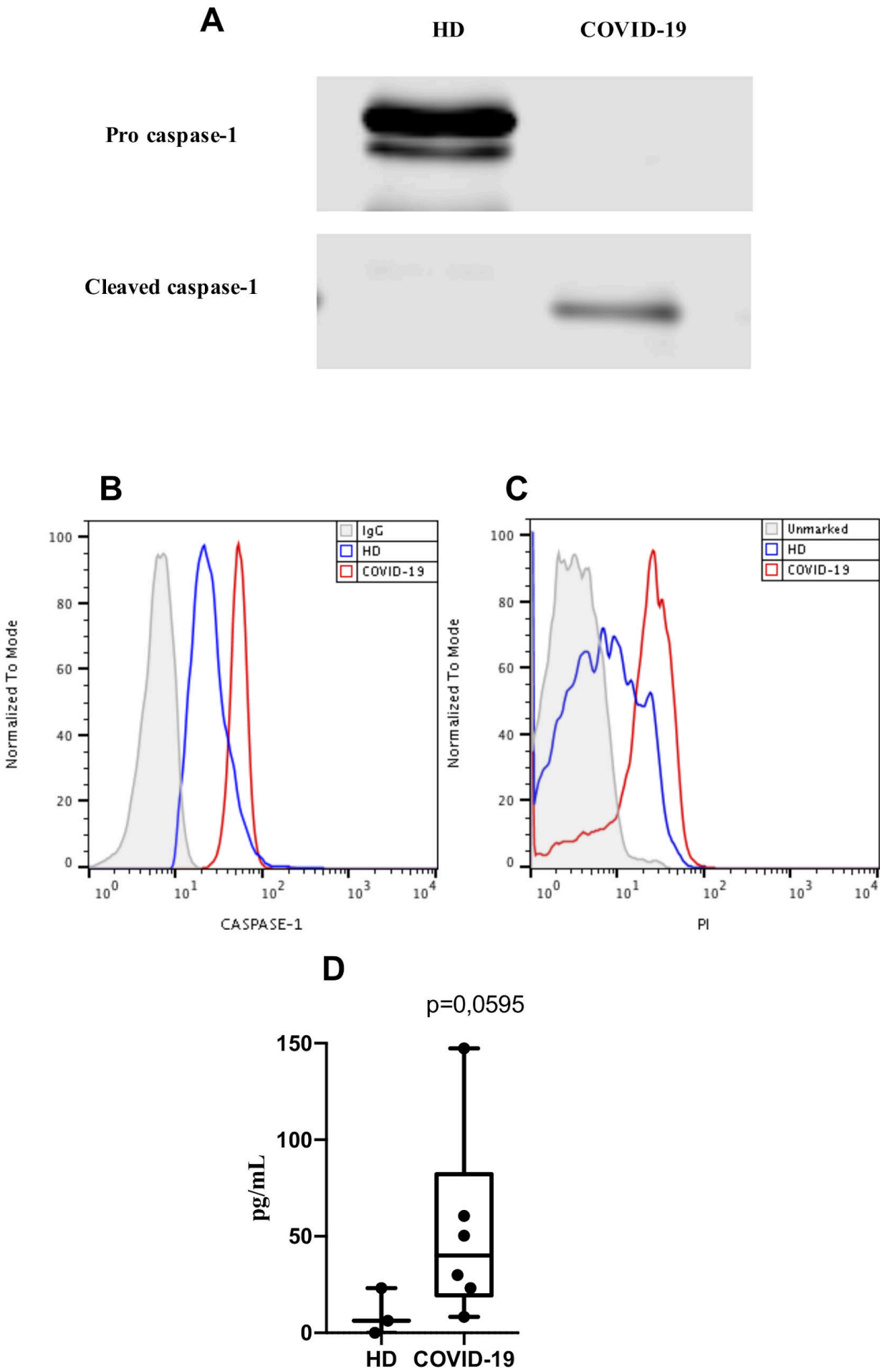
A
HD
COVID-19
Pro caspase-1
Cleaved caspase-1
B
IgG
HD
COVID-19
Normalized To Mode
CASPASE-1
C
Unmarked
HD
COVID-19
Normalized To Mode
PI
D
p=0,0595
pg/mL
HD
COVID-19

FIGURE 7

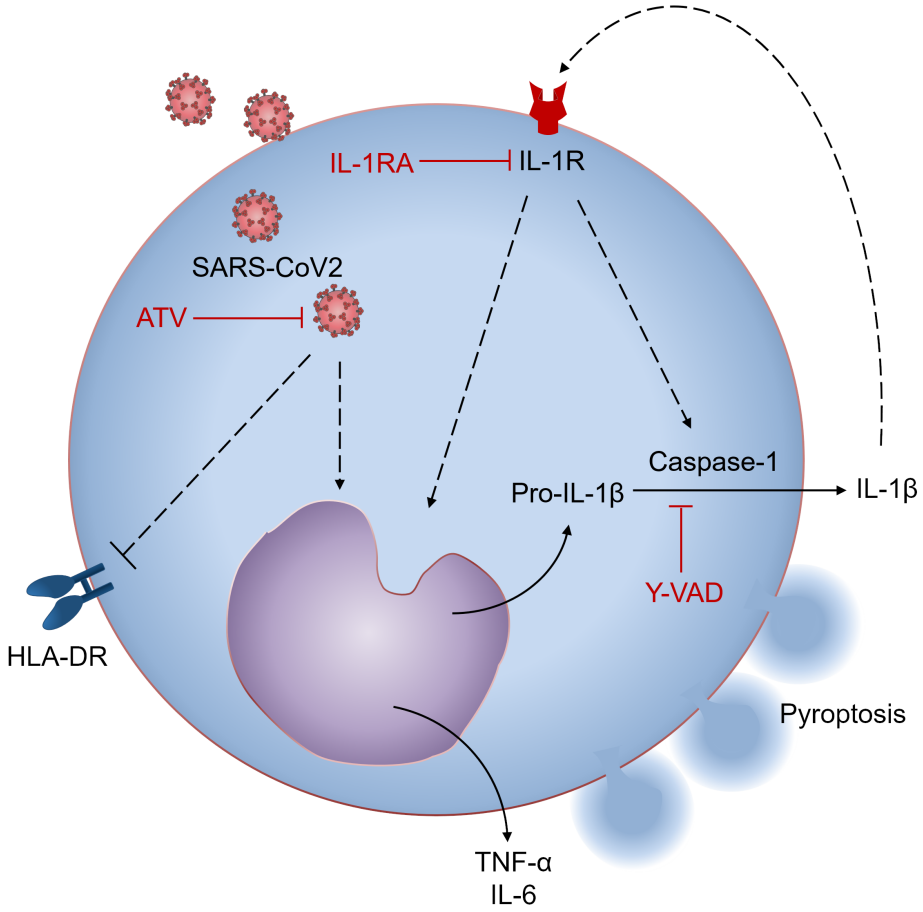
IL-1RA
IL-1R
SARS-CoV2
ATV
Caspase-1
Pro-IL-1β
IL-1β
Y-VAD
HLA-DR
Pyroptosis
TNF-α
IL-6

868 **FIGURE S1**

869
870
871
872
873
874
875
876
877
878
879
880
881
882
883
884

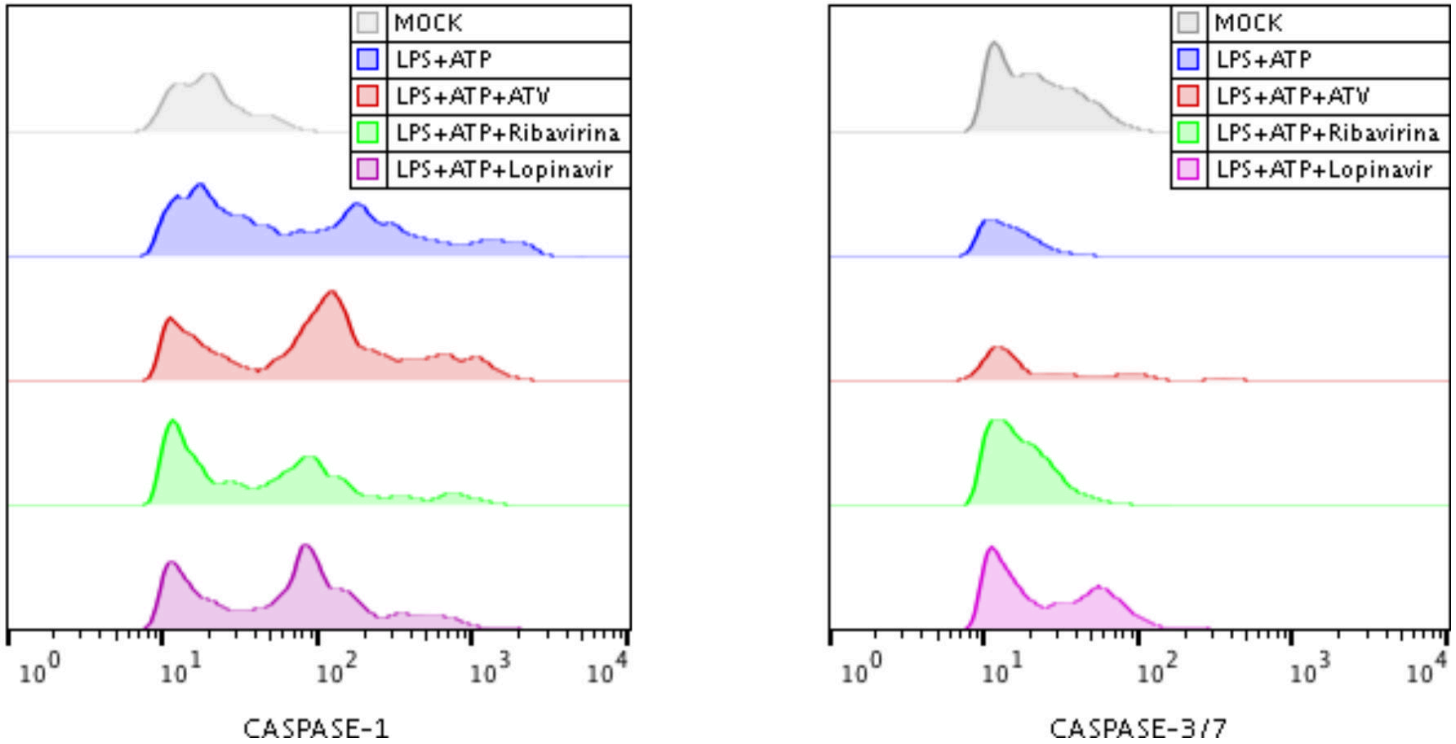

885 **S1 Fig. Evaluation of anti-inflammatory activity of ATV, LPV and ribavirin in LPS-induced monocytes.** Human monocytes were stimulated
886 with LPS (500ng/mL) for 23 h and after this time were stimulated with ATP (2 mM) for 1 h as a positive control group for the formation of
887 inflammasomes and pyroptosis induction. Simultaneously, cells were treated with atazanavir – ATV (10 µM), LPV (10 µM) or ribavirin (10 µM)
888 for 24 h. Monocytes were stained with FAM-YVAD-FLICA (blue) or FAM-FLICA (green) to determine the caspase-1 and caspase-3/7 activity
889 and HLA-DR expression, respectively, and analyzed by flow cytometry. Histograms are representative of six independent experiments.

FIGURE S2

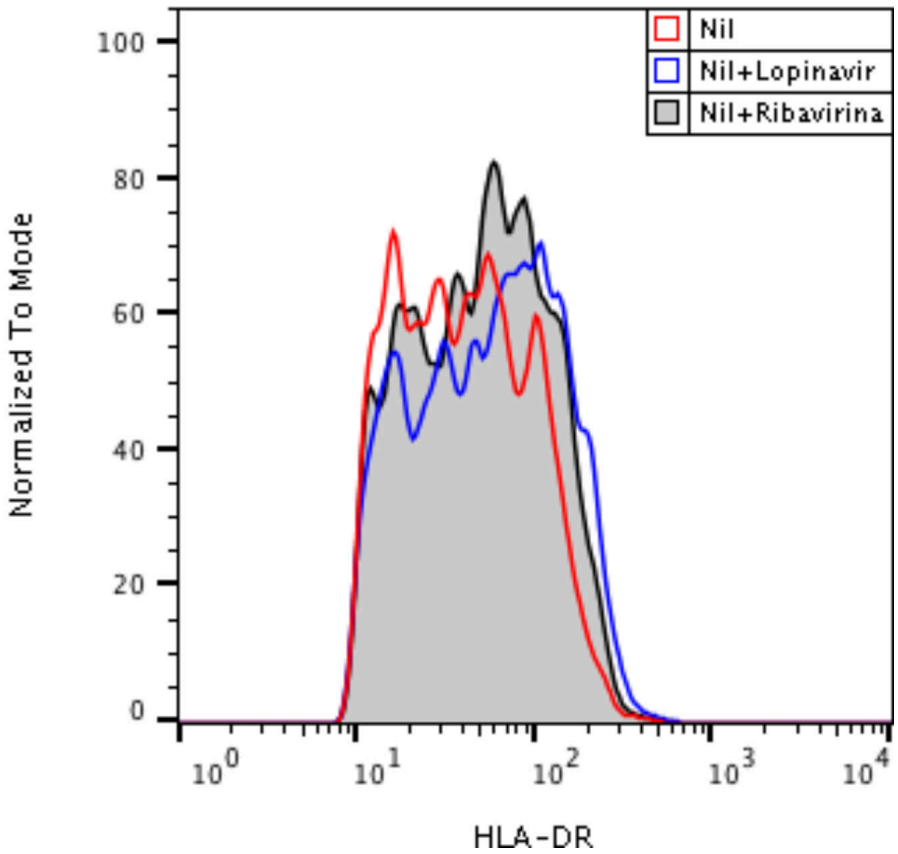

S2 Fig. Effects of LPV and ribavirin in preventing the SARS-CoV-2-related reduced expression of HLA-DR in monocytes. Human monocytes were infected with SARS-Cov-2 and treated with LPV (10 µM) or ribavirina (10 µM) for 24 h. Monocytes were stained with HLA-DR APC.H7 or IgG APC.H7 to determine the HLA-DR expression by flow cytometry. Histogram data are representative of two independent experiments.